Stability Impact of Grid-Tied Photovoltaic Plant on the Distribution Network

Titus O. Ajewole, Olufisayo S. Babalola, Michael O. Omoigui

Abstract— This paper investigates the impact of grid-tied photovoltaic plant on the stability level of the host distribution network. Using simulation model of a grid -connected photovoltaic power system, the response of the distribution sub-system to a test fault experimented on the plant was examined. The behavioural waveforms obtained at three locations across the system reveal the resulting current variations and voltage colapse margins on the network. Subsequent to the removal of the fault however, normal operation was regained by the network, with all the line variables smoothly settled at their initial pre-fault values.

Index Terms— stability, photovoltaic plant, microgrid, distribution network, test fault, behavioural waveform

1 Introduction

PERFORMANCE assessment of distribution networks is a critical requirement for utility reliability in electric power systems. Several cases of voltage collapse and similar power system instabilities are linked to major disturbances such as faults, line switching operations and imbalances between load demand and power supply. Long-term voltage instability can result when a sustained fault condition occurs on the power system, causing it to operate with a reduced capacity over an extended period of time. Various previous works have investigated systems reliability and reliability improvement on the conventional power systems [1], [2]. Using the comprehensive sequential Monte Carlo simulation, [3] evaluated distribution reliability improvement with the installation of dispersed generators.

Over the last few decades however, renewable energy sources such as solar, wind, biomass, small hydropower and fuel-cell have constituted a large part of the distributed generation (DG). The potential of the DG are employed to enhance the overall power system stability. With such growing interest in the adoption of renewable resources, the stability impact of utility-connected DG microgrids on the host grid must be thoroughly investigated. Addition of DG to the existing power distribution system, beyond certain limit and without proper modification and coordination may cause problems on the entire system.

Photovoltaic (PV) technology is a promising alternative source of electricity. One-fifth of the sun's energy falls on land and this is about 2,000 times greater than total present world energy demand at any given time [4], [5]. This alongside with some other reasons account for the significance of the PV conversion of solar radiant energy. However, where PV-based microgrid is connected to the main grid, it may cause improper operation of the grid since PV array experiences large variation in its power output. Some of the issues include voltage regulation, frequency deviation and un-intentional islanding on the system. For optimal utilization of solar electrical resource therefore, and in order to make the technology more operationally safe, PV-based microgrid must be designed to always operate within acceptable voltage limits and ensured it does not have a detrimental effect on the grid operations. Therefore, a study of the effect of PV-based DG on the distribution sub-system is worthwhile. The harmonic interaction between PV plant and distribution network has been investigated [6], while [7] modelled PV system for general performance evaluation with provision for islanding detection and protection. A detail fault-response analysis on grid-integrated PV power system was presented by [8] and, [9] reported a study on the transient characteristics of a grid-interactive PV generator following a disturbance at the generator's terminal.

In this work, the effect of PV-source microgrid on the host distribution sub-system was investigated and reported. The system was implemented using the Simulink/SimPower and the impact of a test fault applied on the microgrid is examined at three locations: at the point of common coupling (PCC) between the microgrid and the main grid; along the distribution line; and at the load terminal. Details of the system modelling and the behavioural waveforms are presented in this paper.

2 Materials and Method

2.1 System Configuration

A model of the complete grid-tied PV system was implemented, with the modelling equations derived from each component segment of the PV plant. The following simplifying assumptions were made in forming the equations:

a) The cells of the PV array are ideal; with neither series loss nor leakage to the ground.
b) All the cells were considered to be equally biased, subjected to the same solar radiation and have the same working temperature.
c) The standard operating conditions (1000W/m² and 300

- *Titus O. Ajewole has the PhD degree in Electronic and Electrical Engineering from the Obafemi Awolowo University, Ile-Ife, Nigeria. PH-2348057235573. E-mail: toajewole2002@yahoo.com*
- *Olufisayo S. Babalola is currently pursuing the PhD degree in Electronic and Electrical Engineering at the Obafemi Awolowo University, Ile-Ife, Nigeria. PH-2348034009873. E-mail: babfisayo@gmail.com*
- *Michael O. Omoigui is currently a Professor of Electronic and Electrical Engineering at the Obafemi Awolowo University, Ile-Ife, Nigeria. PH-2348035017953. E-mail: mikeomoigui@yahoo.co.uk*

Kelvin) were taken as reference.

d) The voltage source inverter (VSI) was of high efficiency with a negligible loss.

The PV plant was connected to the grid via an interface transformer as shown in Figure 1. When exposed to solar radiation, the array generates a sizable amount of direct current (DC) power that is fed to the VSI through a link capacitor. By minimizing the resistive losses over the DC wiring between the array and the inverter, the capacitor stabilizes the input power, thus allowing for a good regulation of the inverter. The inverter converts the DC power fed to its input terminals to alternating current (AC) power obtainable at its output terminals as the switching valves flip the DC power back and forth to create the AC equivalent.

To prevent the spurious voltage output of the inverter's high-frequency switching noises from disturbing the distribution network, a low-pass LC filter is incorporated whose output is serially connected to the primary side of the interface transformer. The ripple-removal recipe of the filter is further enhanced and completed by the inductance of the primary side of the transformer, such that the use of another coupling inductor could be foregone. In addition to its major function of voltage ratio-changing, the transformer also provides galvanic separation between the PV facility and the grid at the point of common coupling of the two. The circuit breaker provides a means of isolating the PV generator from the grid, while a network of 20 km length of power distribution line with a three-phase load connected 3 km way from the PV plant, serves as the distribution.

2.2 Mathematical Description of the System

With the mentioned assumptions, when the PV array has x parallel cell strings with each string having y series-connected cells, the relationship between the output voltage and current of the array is described as follows [10]:

$$I_{pv} = xI_{ph} - xI_{rs}\left[exp\left(\frac{eV_{pv}}{y\sigma kT}\right) - 1\right] \quad (1)$$

I_{mv} and V_{mv} are the current and the voltage output respectively of the PV array and I_{rs} is the reverse saturation current per cell. According to [11], the empirical ideality factor, σ, takes on a value that lies between 1 and 2. The photo-current, I_{ph}, which mainly depends on the solar intensity, S_r and the cell's working temperature, T, is described by:

$$I_{ph} = 0.01[I_{scr} + K_\theta(T - T_r)]S_r \quad (2)$$

Where K_θ and T_r are respectively, the temperature coefficient and the reference temperature. For a single cell, given the open-circuit voltage at the reference condition and the cross-sectional area, A, the short-circuit current at reference, $Iscr$ is determined from the conversion efficiency, η.

$$\eta = \frac{P_{max}}{P_i} = \frac{V_{max}I_{max}}{S_rA} \quad (3)$$

The output power of a cell, expressed in terms of the open-circuit voltage, V_{oc} and the short-circuit current, I_{sc}, is:

$$P_{max} = V_{max}I_{max} = \varphi V_{oc}I_{sc} \quad (4)$$

Where V_{max} and I_{max} are the terminal voltage and the output current respectively of the cell at maximum power point, and φ is the fill-factor, which is a measure of the cell's quality. Therefore, at reference condition:

$$I_{scr} = \frac{\eta AS_r}{\varphi V_{oc}} \quad (5)$$

The reverse saturation current, I_{rs} of a cell varies with its temperature, and it is described by:

$$I_{rs} = I_{rr}\left[\frac{T}{T_r}\right]^3 exp\left[\frac{\varepsilon E}{\sigma k}\left(\frac{1}{T_r} - \frac{1}{T}\right)\right] \quad (6)$$

I_{rr}, which is the reverse saturation current of a cell at the reference temperature and intensity, is obtained by:

$$I_{rr} = \frac{I_{scr}}{exp\left(\frac{\varepsilon V_{oc}}{\sigma kT_r}\right) - 1} \quad (7)$$

For a VSI with Sinusoidal Pulse Width Modulation (SPWM), the modulation ratio, m, the input DC voltage, V and the output voltage, v_t are related by:

$$m = 2\frac{v_t}{V} \quad (8)$$

The VSI's output-side dynamic is described by [12]:

$$v_t = Ri + L\frac{di}{dt} + v_c \quad (9)$$

$$\frac{di}{dt} = -\frac{R}{L}i - \frac{v_c}{L} + \frac{V}{2L}m \quad (10)$$

Where R and L are resistance and inductance of the filter. The modulation index, m in the above model is the control input. In Park's dq frame of reference that rotates synchronously with the grid angular frequency ω, the current dynamics can be represented by the following equations:

$$m_d = \frac{2}{V}\left[Ri_d + L\frac{di_d}{dt} - L\omega i_q + v_{c_d}\right] \quad (11)$$

$$m_q = \frac{2}{V}\left[Ri_q + L\frac{di_q}{dt} + L\omega i_d + v_{c_q}\right] \quad (12)$$

The use of a controller in each axis of the plant to compensate for the non-linearity introduced by ω, enables the system to be operated as a linear plant. With i_d and i_q tracked by reference signals i_{dref} and i_{qref}, the controllers have input error signals e_d and e_q respectively. Therefore, the indexes of the control scheme are:

$$m_d = \left[\{e_d \times H_d(s)\} - L\omega i_q + v_{c_d}\right] \quad (13)$$

$$m_q = \left[\{e_q \times H_q(s)\} + L\omega i_d + v_{c_q}\right] \quad (14)$$

$$H_d(s) = H_q(s) = K_p + \frac{K_i}{S} + K_dS \quad (15)$$

Selection of the filter's inductance L, depends on the current ripple $i_{cr(p-p)}$, the switching frequency and the DC-bus voltage materials It is obtained as [13]:

$$L = \frac{m\sqrt{3}}{12af_si_{cr(p-p)}}V_{dc} \quad (16)$$

The inverter's switching frequency f_s, is measured in hertz, while a is the overload factor. In this study, $i_{cr(p-p)}$ was taken to be 5% as provided by the islanding control standards (IEEE 929-2000). The filter is a low-pass tuned at the grid frequency, with X_C and X_L as capacitive and inductive reactances at the fundamental frequency. Therefore, the filter capacitor is obtained from:

$$1 = \sqrt{\frac{X_C}{X_L}} \quad (17)$$

The three reference signals for the SPWM generator are obtained through Park's inverse-transformation of m_d and m_q as given below:

$$\begin{bmatrix} m_a \\ m_b \\ m_c \end{bmatrix} = \begin{bmatrix} \cos\omega t & -\sin\omega t \\ \cos\left(\omega t - \frac{2\pi}{3}\right) & -\sin\left(\omega t - \frac{2\pi}{3}\right) \\ \cos\left(\omega t - \frac{4\pi}{3}\right) & -\sin\left(\omega t - \frac{4\pi}{3}\right) \end{bmatrix} \begin{bmatrix} m_d \\ m_q \end{bmatrix} \quad (18)$$

The six switching pulses of the VSI are produced by comparing the reference signals m_a, m_b and m_c with the carrier signals of the SPWM generator

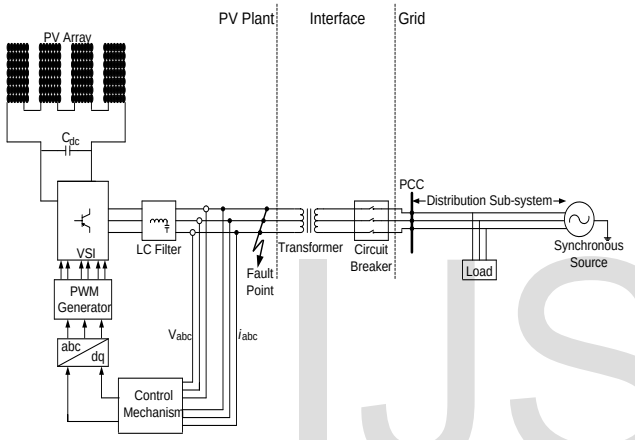

Fig. 1. Utility-Connected Photovoltaic Power System

TABLE
PARAMETERS OF THE SIMULATED DISTRIBUTION NETWORK

Parameters	Values	Units
Line Resistance	0.69	Ω/km/phase
Line Inductance	0.076	mH/km/phase
Line Length	20	Km

3 RESULTS AND DISCUSION

Simulation of the PV array was implemented with the parameters of the commercialized hetero-junction Gallium-Arsenide/Aluminum-Gallium-Arsenide solar cell. The cell provides a relatively good conversion efficiency (24.8%) and operates effectively at elevated temperatures [14]. The simulation lasted for 120 milliseconds, during which a symmetrical short-circuit was demonstrated on the PV plant for a duration of 40milliseconds and the stability response of the distribution network to the disturbance was obtained as waveforms from the three locations.

At the PCC, figure 2 show that the voltage became ideally zero, which consequentially results to a current rise from 10 A to 150A in the effort of the controllers to maintain the pre-set value of the inverter's DC-link voltage. As figure 3 reveals, the current on grid overshoots in the attempt by the system to maintain constant current flow through the distribution line, while the grid voltage however remains undisturbed. Figure 4 shows a 33% drop in the pre-fault values of both the load current and the load voltage.

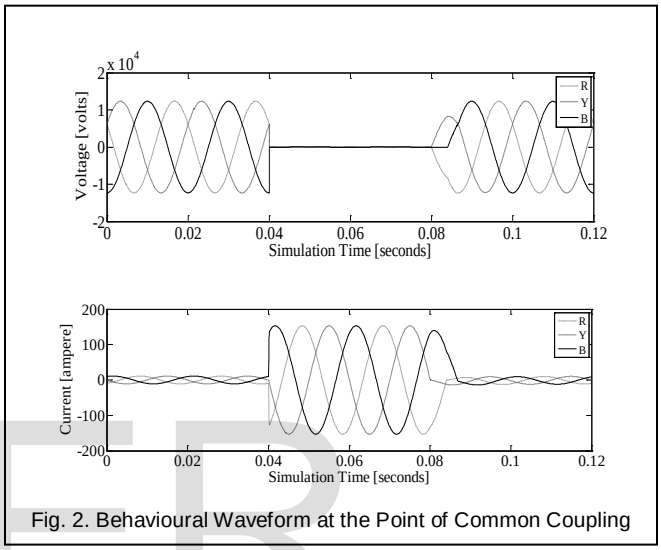

Fig. 2. Behavioural Waveform at the Point of Common Coupling

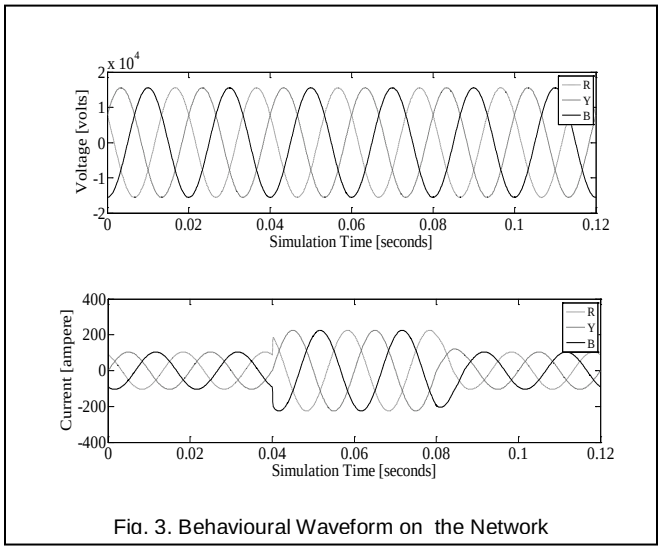

Fig. 3. Behavioural Waveform on the Network

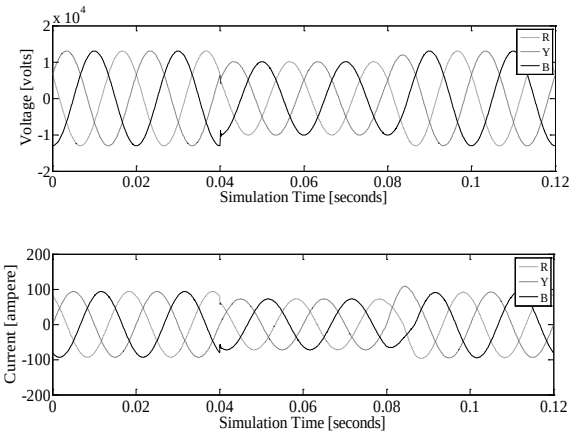

Fig. 4. Behavioural Waveform at the Load Terminal

4 CONCLUSION

Stability impact of PV-source grid-tied DG on the host distribution network has been explored in this study. It is shown through the response obtained from three different locations across the system that a momentary disturbance on the PV plant results into stability failure across the entire distribution network. This therefore indicates that long-term voltage instability can result on the network when a sustained disturbance like fault condition occurs on the PV plant, which can cause the entire system to operate with a reduced capacity over an extended period.

REFERENCES

[1] J.C. Chow, R. Fischil and H. Yan, "On the Evaluation of Voltage Collapse Criteria", *IEEE Transaction on Power System, Vol. 5, No. 2, 1423-1433, 2009.*

[2] N. Hosseinzadeh, Power System Blackouts, " Lessons to Learn", *Proceedings of the Australian Universities on Power Engineering Conference, 2005.*

[3] F. Li and N. Sabir, "Evaluation of Distribution Reliability Improvement with Distributed Generators Using Monte Carlo Simulation", *International Reviews on Modelling and Simulation, Vol. 2, No. 4, 356-361, 2009.*

[4] C.W. Adegoke, P.A. Oluwafisoye, O.K. Ajiboye, and T.O. Ajewole, "Operational Design Parameters in Multi-lamp Module Solar Street Light System", *Nigerian Journal of Solar Energy, Vol. 21, No. 1, 1-8, 2010.*

[5] P.A. Oluwafisoye, C.W. Adegoke, O.K. Ajiboye, and T.O. Ajewole, "Development of a 3.5kW Solar Power Pack Dedicated to Laboratory Equipment at Osun State University, Osogbo, Nigeria", *Nigerian Journal of Solar Energy, Vol. 21, No. 1, 9-14, 2010.*

[6] G.A. Abou-Khalil, D.C. Lee, J.K. Seok, J.W. Choi and H.G. Kim, "Maximum Power Point Tracking Controller Connecting PV System to Grid", School of Electrical Engineering and Computer Science, Yeungnam University,Korea, 2005.

[7] P.P. Dash and A. Yazdani, "Mathematical Modeling and Performance Evaluation of a Single-Stage Grid-Connected Photovoltaic System", *International Journal of Emerging Electric Power, Vol. 9,* Issue 6, *1-32, 2008.*

[8] T.O. Ajewole, "*Fault Analysis on Grid-Integrated Photovoltaic Power System*", Master of Science Thesis, Department of Electronic and Electrical Engineering, Obafemi Awolowo University, Ile-Ife Nigeria, 2010.

[9] M.O. Omoigui, T.O. Ajewole and F.K. Ariyo, "Investigation of the Transient Behaviour of Grid-Connected Photovoltaic Power Generator", *NSE Transaction, Vol. 46, No. 1, 97 – 107, 2011.*

[10] M. Nikraz, H. Dehbonei and C. Nayar, "A DSP-Controlled Photovoltaic System with Maximum Power Point Tracking", Center for Renewable Energy and Sustainable Technologies, Australia, 2003.

[11] G.N. Tiwari, "*Solar Energy Fundamentals: Designs, Modeling and Applications*", (Narosa Publishing House, 2002).

[12] H.M. Ryu, J.H. Kim and S.K. Sul, "Analysis of Multiphase Space Vector Pulse-Width Modulation Based on *dq* Space Concept", *IEEE Transactions on Power Electronics, Vol. 20, No. 6, 1364-1371, 2005.*

[13] B. Singh, P. Jayaprakash and D.P. Kothari, "A T-Connected Transformer and Three-Leg VSC-Based DSTATCOM for Power Quality Improvement", *IEEE Transactions on Power Electronics, Vol. 23, No. 6, 1364-1371, 2008.*

[14] B.G. Streetman and S.K. Banerjee, "*Solid State Electronic Devices*", (Pearson Education Incorporated, 2006).